Thermodynamic study of a phase-change solvent: New experimental data and modelling

Y. Coulier, K. Ballerat-Busserolles, L. Rodier, J-Y. Coxam

Thermodynamic study of a phase-change solvent: new experimental data and modelling

Y. Coulier[a*], K. Ballerat-Busserolles[a], L. Rodier[a], J-Y. Coxam[a]

[a]Université Clermont Auvergne, CNRS, SIGMA Clermont, Institut de Chimie de Clermont-Ferrand, F-63000 Clermont-Ferrand, France

[*] To whom correspondence should be addressed.
Tel + 33 473407196. Fax + 33 473405328 E-mail: yohann.coulier@uca.fr

Abstract

The 2,4,6-tris(dimethylaminomethyl)phenol shows a partial miscibility with water. The temperatures of liquid-liquid phase separation were experimentaly determined to establish the phase diagram. The specific heat capacities and densities of aqueous solutions of 2,4,6-tris(dimethylaminomethyl)phenol were measured to determine excess heat capacities and excess molar volume. Experiments have been carried out for temperatures range from 288 K to 338 K, at atmospheric pressure. The NRTL model was used to correlate liquid-liquid equilibria and, the UNIQUAC model to correlate heat capacities and predict excess molar enthalpies. The excess molar volumes were fitted to a Redlich–Kister polynomial.

Keywords : density; liquid-liquid equilibrium; specific heat capacity; thermodynamic modeling; excess enthalpy.

1. Introduction

Separation of multicomponent gases using absorption/desorption cycles in aqueous solutions of amine is a very well-known and efficient method used for the treatment of natural gas. Aqueous solutions of alkanolamine are efficient solvent for CO_2 removal. Nevertheless, a critical disadvantage of the process using these conventional amines is the energy costs for solvent regeneration. New processes using phase change solvents are aimed at addressing this issue [1, 2]. These solvents undergo a liquid-liquid phase separation depending on temperature and CO_2 charge loading. A phase separation unit could be integrated in the process to limit the energetic cost of the solvent regeneration step by lowering the amount of absorbent to be treated and reducing the energy requirements. The absorbents used in the DMX™ process developed by IFP Energies Nouvelles [1-4], are aqueous solutions of amine capable of phase separation according to particular conditions of temperatures (higher than the absorption temperature) and CO_2 loading charges in order to avoid any liquid-liquid mass transfer limitation [1].

The selection of suitable amines for these new processes requires a complete study of their thermo-physical properties in aqueous solutions. This includes phase equilibrium diagrams as well as transport and energetic properties. Thermodynamic models capable of reproducing phase equilibria and energetic properties (i.e., enthalpies and heat capacities of the flowing {amine + water} mixtures) are required to develop such a process. However to develop these models, experimental data are an imperious prerequisite. The present investigation combines the acquisition of experimental data and thermodynamic modelling of a new a phase change solvent.

This work provides experimental data of liquid-liquid equilibrium (LLE) for aqueous solutions of 2,4,6-tris(dimethylaminomethyl)phenol (DMP-30), as well as excess heat capacities (C_p^E) and excess volumes (V^E). No thermodynamic data were found in the literature for this new demixing solvent. LLE were determined using a calorimetric technique. Measurements were carried out up to 343K using a micro differential scanning calorimetry (MicroDSC III from Setaram). LLE were also determined by direct visualization using an equilibrium cell SPM20 from Thar Technologies. This second technique permits to validate the calorimetric technique and to extend temperature domain of investigation up to 393 K. C_p^E were determined at 0.1 MPa and at 298.15 K and 308.15 K from the heat capacities (C_p) of pure amines and aqueous solutions, which were measured with the MicroDSC III. V^E were derived from density data. The density measurements were performed at 0.1 MPa and at

temperatures ranging from 288.15K to 308.15K using a Sodev-Picker vibrating tube densimeter.

The study also proposes the use of thermodynamic models that can represent experimental data, including phase diagrams. The NRTL and UNIQUAC activity coefficient models led to an acceptable reproduction of the thermodynamic properties stemming from this work. The combination of these experimental and theoretical tools are adapted for a general characterization of the demixing solvents and the analysis of their potentials use for acid gas capture processes.

2. Experimentals

2.1 Materials

2,4,6-tris(dimethylaminomethyl)phenol (DMP-30, CAS 90-72-2) is used without further purification. The water content of pure DMP-30 was measured using a Coulometric Karl-Fischer titrator (Mettler Toledo, DL31). The measured water content was accounted for upon amine solutions preparation. NaCl(s) (ACS reagent), was dried in an oven overnight at T = 523.15 K, stored in a dessicator containing P_2O_5, and re-dried before use. Water is distilled and degassed under vacuum before use. Aqueous solutions are prepared by mass. Aqueous solutions of amine were stored in glass bottle in an opaque cabinet to prevent any photo-degradation. Suppliers, purities of all chemicals used in this study and the water content of pure DMP-30 are given in Table 1.

2.2 Techniques

2.2.1 Differential scanning calorimeter

The experimental technique to measure heat capacities and liquid-liquid equilibria were described in details by Coulier et al. [5, 6]. Isobaric heat capacities and liquid-liquid equilibria were determined using a Setaram MicroDSC III differential scanning calorimeter. The instrument was calibrated for temperature accuracy using naphthalene. Experiments are carried out with one milliliter liquid Cp cells. The sample cell is filled with the binary {amine – water} mixture and the reference cell is filled with water. Cells are kept connected through capillary tubes to reservoir syringes maintained at atmospheric pressure. The experiments are performed at constant pressure with no vapor phase in the cell. The experimental protocol consists in running sequences of 10 minutes isothermal step at 283 K, 140 minutes heating

scan at 0.5 K·min^{-1} up to 353 K and, 10 minutes isothermal step at 353 K. The general appearances of the thermograms obtained for an aqueous solution of amine or for pure water are shown in Figure 2 of [6]. The liquid-liquid phase separation is indicated on the thermogram by a weak exothermic peak. The temperatures of liquid-liquid separation reported in this work correspond to the onset point of the peak. The uncertainty on the temperatures of phase separation, determined from reproducibility tests, is estimated about 2 K.

The differential baseline signal, recorded below the temperature of liquid-liquid separation is proportional to heat capacity difference between reference and sample cells. Thus the specific heat capacity ($c_{p,s}$) of a solution is obtained with eq. 1.

$$\rho_s c_{p,s} = \rho_w c_{p,w} + K_T[(\mathrm{d}Q/\mathrm{d}t)_s - (\mathrm{d}Q/\mathrm{d}t)_w] \quad (1)$$

where $(\mathrm{d}Q/\mathrm{d}t)_s - (\mathrm{d}Q/\mathrm{d}t)_w$, is the difference of differential thermal flux recorded with the measuring cell successively filled with the solution and water. The specific heat capacity ($c_{p,w}$) and the density of pure water (ρ_w) are obtained from Hill [7]. The densities of aqueous solution of amine (ρ_s) were measured using a Sodev Picker vibrating tube densimeter (section 2.2.3). The calibration constant K_T in equation 1 is determined from measurement carried out with NaCl aqueous solutions of well-known isobaric heat capacities [8]. The uncertainty for specific heat capacity $c_{p,s}$ is mainly due to the uncertainty on solutions densities and the reproducibility of the heat flux signals. Including, the uncertainty on isobaric heat capacity of water and calibration constant, the relative uncertainty of $c_{p,s}$ is estimated to be 0.6 %.

2.2.2 Liquid-liquid equilibrium cell

A phase equilibrium cell SPM20 from Thar Technologies was used to validate the calorimetric technique described above and to determine the liquid-liquid phase diagram at temperatures T > 350 K. The experimental equipment was described elsewhere [9]. The solution is introduced in a high pressure chamber equiped with a thick sapphire window. A heat tape surrounding the body vessel allowins a progressive and uniform heating of the chamber. The stirring inside the chamber is insured by a spherical magnet driven from the exterior. The experimental protocol consists in steeply increasing temperature by small increments in order to insure temperature homogeneity inside the high pressure chamber. The phase separation is visually determined when clear solution (monophasic) goes through a cloud point (diphasic solution). The uncertainty on the temperature of cloud point estimated

from reproducibility tests is less than 2 K while uncertainty on such temperature determination for one experiment is better than 0.4 K.

2.2.3 Densimeter

The densities of {amine – water} systems ρ_s and pure amine ρ_a were determined at atmospheric pressure using a Sodev Picker vibrating tube densimeter. The experimental procedure was previously described [6]. Measurements are carried out at temperatures ranging from 288.15 K to 338.15 K, for amine molar fractions x_a selected within the one phase region. Precision on temperature is 0.03 K. The densities are calculated using equation 2 where τ_s and τ_w represent the tube vibration periods when flowing aqueous solution of amine and pure water, respectively. Pure water is used as reference fluid with densities ρ_w obtained from Hill [7]. The densimeter calibration constant K_d in equation 2 is determined at given temperature by running experiments with NaCl aqueous solutions of well-known densities [8].

$$\rho_s = \rho_w + K_d(\tau_s^2 - \tau_w^2) \quad (2)$$

Literature and experimental values of densities calculated with the adjusted calibration constant for aqueous solutions of sodium chloride are given in Table 2. The relative standard uncertainty on pure DMP-30 is 0.5 % due to its low purity [10].

3. Results and Discussion

3.1 Temperatures of liquid-liquid phase separation

The LLE diagram (T, x_a) of {water - DMP-30} system was determined for amine molar fraction up to x_a = 0.34. The temperatures of liquid-liquid phase separation as function of amine molar fraction x_a are reported in Table 3 and represented in Figure 1. The diagram exhibits a lower critical solution temperature (LCST) at 317.3 K and amine molar fraction x_a=0.03.

The LLE experimental data (temperature of phase separation as function of amine molar fraction) were correlated using two models. First, the extended scaling law equation was employed to smooth the experimental data (Table 3). Second, the NRTL model was used to represent LLE from the excess Gibbs energy of {DMP-30 – water} system.

The extended scaling law equation (eq. 3a-3b) [11, 12] was used to fit the binodal curve of {DMP-30 – water} system. This model provides 2 expressions for the amine molar fraction as

function of phase separation temperature (T), one in the amine rich phase (x_a^a) and second one in the water rich-phase (x_a^w).

$$x_{\mathrm{a}}^{\mathrm{a}} = x_{\mathrm{ca}} - B_1|1 - T/T_{\mathrm{c}}|^{\beta} - B_2|1 - T/T_{\mathrm{c}}|^{\beta+w} + A_1|1 - T/T_{\mathrm{c}}| - B_3|1 - T/T_{\mathrm{c}}|^{\beta+2w} + A_2|1 - T/T_c|^{1-\alpha+w} \quad (3a)$$

and

$$x_{\mathrm{a}}^{\mathrm{w}} = x_{\mathrm{ca}} + B_1|1 - T/T_{\mathrm{c}}|^{\beta} + B_2|1 - T/T_{\mathrm{c}}|^{\beta+w} + A_1|1 - T/T_{\mathrm{c}}| + B_3|1 - T/T_{\mathrm{c}}|^{\beta+2w} + A_2|1 - T/T_{\mathrm{c}}|^{1-\alpha+w} \quad (3b)$$

The lower critical solution temperature (T_{c}) and molar fraction of the critical point x_{ca}, were adjusted along with parameters A_i and B_i by regression of the LLE experimental data. The parameters α, β and w, whose original meaning can be found in the literature [12-14], were set as follows: α = 0.11, β = 0.329 and w=0.5. The regression of the scaling law equation parameters was performed using Minuit software [15]. The function Simplex was used to optimize these parameters using the normalized objective function F_1 expressed in equation 4.

$$F_1 = \sum_i^{n_{exp}} \left(\frac{x_{\mathrm{a},i}^{\mathrm{a,exp}} - x_{\mathrm{a},i}^{\mathrm{a,calc}}}{x_{\mathrm{a},i}^{\mathrm{a,exp}}} \right)^2 + \left(\frac{x_{\mathrm{a},i}^{\mathrm{w,exp}} - x_{\mathrm{a},i}^{\mathrm{w,calc}}}{x_{\mathrm{a},i}^{\mathrm{w,exp}}} \right)^2 \quad (4)$$

The resulting parameters are listed in Table 4 and T_{c} and x_{ca} are found to be 317.50 K and 0.0250 respectively.

The NRTL model [16] was employed to represent the excess Gibbs energy. The model interaction parameters $\tau_{ij}^{\mathrm{NRTL}}$ (Eq.5) and a_{ij}^{NRTL} (Eq. 6) were assumed to be temperature dependent; indices 1, 2 refer to amine and water, respectively.

$$\tau_{12}^{\mathrm{NRTL}} = \frac{a_{12}^{\mathrm{NRTL}}}{T} \quad \text{and} \quad \tau_{21}^{\mathrm{NRTL}} = \frac{a_{21}^{\mathrm{NRTL}}}{T} \quad (5)$$

$$\begin{cases} a_{12}^{\mathrm{NRTL}} = A_{12}^{\mathrm{NRTL}} + B_{12}^{\mathrm{NRTL}} T + C_{12}^{\mathrm{NRTL}} T^2 \\ a_{21}^{\mathrm{NRTL}} = A_{21}^{\mathrm{NRTL}} + B_{21}^{\mathrm{NRTL}} T + C_{21}^{\mathrm{NRTL}} T^2 \end{cases} \quad (6)$$

The NRTL parameters, $A_{i,j}^{\mathrm{NRTL}}$, $B_{i,j}^{\mathrm{NRTL}}$ and $C_{i,j}^{\mathrm{NRTL}}$, were calculated by solving equations describing the phase equilibrium as the equality of the component activities in the conjugated liquid phases. These parameters were optimized by regression of a LLE data generated by equations 3a and 3b and parameters in Table 4; amine molar fractions in water and amine rich phases were calculated at temperatures covering the experimental temperature range [317 K – 353 K] with 1 K increment. A Fortran code based on the algorithm developed by Privat *et al.* [17] was used for the calculations. All the parameters in equation 6 are summarized Table 4 and the correlation of the LLE data is illustrated in Figure 1.

3.2 Isobaric molar heat capacities and excess molar heat capacities

Experimental specific heat capacities of pure DMP-30 ($c_{p,a}$) were measured from 298.15 K to 338.15 K and are reported in Table 5.

The molar heat capacities $C_{p,s}$ of {DMP-30 – water} system were measured for different amine mole fractions (x_a) at temperatures below the LCST. Excess molar heat capacities (C_p^E) at 298.15 and 308.15 K, were derived (eq. 7) from the experimental molar heat capacities of pure amine ($C_{p,a}$), pure water ($C_{p,w}$) and aqueous solution of amine ($C_{p,s}$).

$$C_p^E = C_{p,s} - \left(x_a C_{p,a} + x_w C_{p,w}\right) \tag{7}$$

The molar heat capacities and molar excess heat capacities of {DMP-30 – water} systems are reported in Table 6. Excess molar heat capacities are represented as function of composition in Figure 2. The uncertainties on C_p^E in Table 6 were estimated using basic principles of error propagation in eq 7.

Excess molar heat capacity C_p^E was observed to be positive and, to increase with temperature. Positive C_p^E implies destruction of liquid structure as temperature is raised [18], which is in agreement with the fact that {DMP – water} system undergo a LCST. The large positive values of C_p^E may be ascribed to measurements conducted at temperatures close to the LCST.

The experimental data of molar excess heat capacities were used to adjust parameters in the original UNIQUAC model developed by Abrams and Prausnitz [19], modified by Anderson and Prausnitz [20]. The excess Gibbs energy excess is considered (Eq. 8) as the sum of a combinatorial and a residual terms.

$$\frac{G^E}{RT} = \left(\frac{G^E}{RT}\right)^{\text{comb}} + \left(\frac{G^E}{RT}\right)^{\text{res}} \tag{8}$$

The molar excess heat capacities are derived from molar excess enthalpies (H^E) (Eq. 9) and the molar excess enthalpy is obtained from the Gibbs free energy (G^E), following the Gibbs–Helmholtz equation (Eq. 10).

$$c_p^E = \left(\frac{\partial H^E}{\partial T}\right)_{p,n} \tag{9}$$

$$-\frac{H^E}{RT^2} = \left(\frac{\partial\left(G^E/RT\right)}{\partial T}\right)_{p,n} \tag{10}$$

The original UNIQUAC model includes volume parameters (r_i), surface parameters (q_i , q_i')

and interaction energy parameters ($\tau_{ij}^{\mathrm{UNIQUAC}}$). The temperature dependence of the interaction parameters (Eq. 11) were expressed following equations 11 and 12.

$$\tau_{12}^{\mathrm{UNIQUAC}} = \exp\left(-\frac{a_{12}^{\mathrm{UNIQUAC}}}{T}\right) \quad \text{and} \quad \tau_{21}^{\mathrm{UNIQUAC}} = \exp\left(-\frac{a_{21}^{\mathrm{UNIQUAC}}}{T}\right) \tag{11}$$

The temperature dependences of the energy parameters a_{ij} were expressed by a quadratic function of temperature:

$$\begin{cases} a_{12}^{\mathrm{UNIQUAC}} = A_{12}^{\mathrm{UNIQUAC}} + B_{12}^{\mathrm{UNIQUAC}} T + C_{12}^{\mathrm{UNIQUAC}} T^2 \\ a_{21}^{\mathrm{UNIQUAC}} = A_{21}^{\mathrm{UNIQUAC}} + B_{21}^{\mathrm{UNIQUAC}} T + C_{21}^{\mathrm{UNIQUAC}} T^2 \end{cases} \tag{12}$$

Coefficients $A_{i,j}^{\mathrm{UNIQUAC}}$, $B_{i,j}^{\mathrm{UNIQUAC}}$ and $C_{i,j}^{\mathrm{UNIQUAC}}$ in equation 12 were simultaneously determined by fitting both the $C_{\mathrm{p}}^{\mathrm{E}}$ data and VLE data from Dergal [21] for {DMP-30 – water} system. The optimization of the coefficients was performed using the objective function reported in equation 13; function F was minimized using the simplex function in Minuit software.

$$F = 100\left(\frac{1}{n_1}\sum_i^{n_1}\left|\frac{C_{p,i}^{E,exp} - C_{p,i}^{E,cal}}{C_{p,i}^{E,exp}}\right| + \frac{1}{n_2}\sum_i^{n_2}\left|\frac{p_i^{exp} - p_i^{cal}}{p_i^{exp}}\right|\right) \tag{13}$$

All UNIQUAC model parameters are resumed in Table 4. Excess molar enthalpies of {DMP30 – H_2O} system were calculated with the optimized UNIQUAC model at 298.15 K and 308.15 K. The predicted excess molar enthalpies are illustrated in Figure 3. The mixing of DMP-30 with water was found to be an exothermic reaction with minimum values at amine molar fraction $x_a \approx 0.31$, -2900 J.mol^{-1} at 298.15 K and -2700 J.mol^{-1} at 308.15K. These values are consistent with the creation of strong hydrogen bond in the solution and, are in same order of magnitude than those found for alkanolamines and water systems [22, 23].

3.3 Densities and excess molar volumes

The experimental densities of pure DMP-30 (ρ_a) were determined from 288.15 K to 338.15 K and are reported in table 5. The experimental and the available literature data are compared graphically in Figure 4. At 288.15 K the observed deviation of 1.4 % with Bruson and MacMullen [24] data is greater than the experimental standerd uncertainty. The density data reported by Bondi and Parry [25] at 303.15 K appears to be in a good agreement with the temperature trend of the experimental density of pure DMP-30.

The densities (ρ_s) of aqueous solution of DMP-30 were measured at temperatures below the LCST i.e. at temperature range from 288.15 K to 308.15 K. The excess molar volumes V^{E}

were derived (Eq. 14) from density data and the molar mass of pure amine (M_a) and pure water (M_w). Standard uncertainty on molar fraction, density and excess molar volumes are calculated using basic principles of error propagation.

$$V^E = \frac{x_{\mathrm{w}}\mathrm{M}_{\mathrm{w}}+x_{\mathrm{a}}\mathrm{M}_{\mathrm{a}}}{\rho_{\mathrm{s}}} - \left(\frac{x_{\mathrm{w}}\mathrm{M}_{\mathrm{w}}}{\rho_w} + \frac{x_{\mathrm{a}}\mathrm{M}_{\mathrm{a}}}{\rho_a}\right) \quad (14)$$

Experimental densities (ρ_s) and excess molar volumes (V^E) for {DMP-30 – water} system are reported in Table 7 and, represented as function of composition in Figures 5.

The large negative V^E values are consistent with the large and negative predicted H^E indicating the existence of strong interactions between unlike molecules.

The excess molar volumes were fitted to a Redlich-Kister polynomial (Eq. 15); three adjustable parameters were sufficient to correctly fit the excess molar volumes. The parameters a_i in equation 15 and, standard deviation σ, are reported in Table 8.

$$V^E = x_{\mathrm{w}}x_{\mathrm{a}}\sum_{i=0}^{n} a_i(x_{\mathrm{w}} - x_{\mathrm{a}})^i \quad (15)$$

For each temperature, the curves show negative excess molar volumes with a minimum value at amine molar fraction x_a around 0.27. The extrema for excess heat capacity; enthalpy and volume were all found around same amine molar fraction x_a = 0.3. Negative excess molar volumes corroborate the existence of strong hydrogen bond in {DMP-30-water} systems; absolute value of V^E slightly decreases with temperature as hydrogen-bonds are weakened.

4. Conclusion

This work have presented experimental techniques for the determination of temperature of liquid-liquid phase separation, heat capacities and densities for {amine - water} system. The excess molar heat capacities and molar volume, derived from experimental data, indicate the existence of hydrogen bond in amine – water systems. For DMP-30, a liquid-liquid phase separation was observe when increasing temperature, with a LCST at 317.3 K and amine molar fraction x_a=0.03. The NRTL activity coefficient model, combine with an extended scaling law equation, can be used to correctly represent the phase diagram. The excess enthalpy can be derived from heat capacity data using UNIQUAC model. The excess enthalpy corresponds to the enthalpy of mixing amine with water, an energetic property of interest for process design. To the best of our knowledge, this paper is the first study on the thermodynamic properties of DMP-30. This procedure can be applied to analyse the potential of aqueous solutions of amine as a demixing solvent in Carbon dioxide capture process. These

works must then be completed by a study of gas absorption and its influence on the temperatures of liquid-liquid phase separation.

Acknowledgement
This work was carried out within the ACACIA project which is funded by DGE (French General Directorate for Entreprise), Grand Lyon and AXELERA.

References

1. M. Aleixo, M. Prigent, A. Gibert, F. Porcheron, I. Mokbel, J. Jose, M. Jacquin
Physical and chemical properties of DMX™ solvents
Energy Procedia, 4 (2011), pp. 148-155
DOI: http://dx.doi.org/10.1016/j.egypro.2011.01.035.

2. L. Raynal, P. Alix, P.-A. Bouillon, A. Gomez, M. le Febvre de Nailly, M. Jacquin, J. Kittel, A. di Lella, P. Mougin, J. Trapy
The DMX™ process: An original solution for lowering the cost of post-combustion carbon capture
Energy Procedia, 4 (2011), pp. 779-786
DOI: http://dx.doi.org/10.1016/j.egypro.2011.01.119.

3. L. Raynal, P.-A. Bouillon, A. Gomez, P. Broutin
From MEA to demixing solvents and future steps, a roadmap for lowering the cost of post-combustion carbon capture
Chemical Engineering Journal, 171 (2011), pp. 742-752
DOI: http://dx.doi.org/10.1016/j.cej.2011.01.008.

4. L. Raynal, P. Briot, M. Dreillard, P. Broutin, A. Mangiaracina, B.S. Drioli, M. Politi, C. La Marca, J. Mertens, M.-L. Thielens, G. Laborie, L. Normand
Evaluation of the DMX Process for Industrial Pilot Demonstration – Methodology and Results
Energy Procedia, 63 (2014), pp. 6298-6309
DOI: http://dx.doi.org/10.1016/j.egypro.2014.11.662.

5. Y. Coulier, K. Ballerat-Busserolles, J. Mesones, A. Lowe, J.-Y. Coxam
Excess Molar Enthalpies and Heat Capacities of {2-Methylpiperidine–Water} and {N-Methylpiperidine–Water} Systems of Low to Moderate Amine Compositions
Journal of Chemical & Engineering Data, 60 (2015), pp. 1563-1571
DOI: 10.1021/je5008444.

6. Y. Coulier, K. Ballerat-Busserolles, L. Rodier, J.Y. Coxam
Temperatures of liquid–liquid separation and excess molar volumes of {N-methylpiperidine–water} and {2-methylpiperidine–water} systems
Fluid Phase Equilibria, 296 (2010), pp. 206-212
DOI: https://doi.org/10.1016/j.fluid.2010.05.001.

7. P.G. Hill
A Unified Fundamental Equation for the Thermodynamic Properties of H2O
Journal of Physical and Chemical Reference Data, 19 (1990), pp. 1233-1274
DOI: 10.1063/1.555868.

8. D.G. Archer
Thermodynamic Properties of the NaCl+H2O System. II. Thermodynamic Properties of NaCl(aq), NaCl·2H2(cr), and Phase Equilibria
Journal of Physical and Chemical Reference Data, 21 (1992), pp. 793-829
DOI: 10.1063/1.555915.

9. Y. Coulier, A.R. Lowe, A. Moreau, K. Ballerat-Busserolles, J.Y. Coxam
Liquid-liquid phase separation of {amine – H2O – CO2} systems: New methods for key data
Fluid Phase Equilibria, 431 (2017), pp. 1-7
DOI: https://doi.org/10.1016/j.fluid.2016.10.010.

10. R.D. Chirico, M. Frenkel, J.W. Magee, V. Diky, C.D. Muzny, A.F. Kazakov, K. Kroenlein, I. Abdulagatov, G.R. Hardin, W.E. Acree, J.F. Brenneke, P.L. Brown, P.T. Cummings, T.W. de Loos, D.G. Friend, A.R.H. Goodwin, L.D. Hansen, W.M. Haynes, N. Koga, A. Mandelis, K.N. Marsh, P.M. Mathias, C. McCabe, J.P. O'Connell, A. Pádua, V. Rives, C. Schick, J.P.M. Trusler, S. Vyazovkin, R.D. Weir, J. Wu
Improvement of Quality in Publication of Experimental Thermophysical Property Data: Challenges, Assessment Tools, Global Implementation, and Online Support
Journal of Chemical & Engineering Data, 58 (2013), pp. 2699-2716
DOI: 10.1021/je400569s.

11. D. Shaw, A. Skrzecz, J.W. Lorimer, A. Maczynski (eds)
Alcohols with Hydrocarbons, IUPAC Solubility Data Series Vol. 56
Oxford University Press (1994)

12. M.B. Ewing, K.A. Johnson, M.L. McGlashan
The (liquid + liquid) critical state of (cyxlohexane + methanol) IV. (T, x)p coexistence curve and the slope of the critical line
The Journal of Chemical Thermodynamics, 20 (1988), pp. 49-62
DOI: https://doi.org/10.1016/0021-9614(88)90209-1.

13. M. Ley-Koo ,M.S. Green
Consequences of the renormalization group for the thermodynamics of fluids near the critical point
Physical Review A, 23 (1981), pp. 2650-2659
DOI: 10.1103/PhysRevA.23.2650.

14. R.R. Singh ,W.A.V. Hook
Comments on classical and nonclassical representations of critical demixing in liquid–liquid binary solutions
The Journal of Chemical Physics, 87 (1987), pp. 6088-6096
DOI: 10.1063/1.453483.

15. F. James ,M. Roos
Minuit - a system for function minimization and analysis of the parameter errors and correlations
Computer Physics Communications, 10 (1975), pp. 343-367
DOI: http://dx.doi.org/10.1016/0010-4655(75)90039-9.

16. H. Renon ,J.M. Prausnitz
Local compositions in thermodynamic excess functions for liquid mixtures
AIChE Journal, 14 (1968), pp. 135-144

DOI: doi:10.1002/aic.690140124.

17. R. Privat, J.-N. Jaubert, Y. Privat
A simple and unified algorithm to solve fluid phase equilibria using either the gamma–phi or the phi–phi approach for binary and ternary mixtures
Computers & Chemical Engineering, 50 (2013), pp. 139-151
DOI: https://doi.org/10.1016/j.compchemeng.2012.11.006.

18. D. Patterson
Structure and the thermodynamics of non-electrolyte mixtures
Journal of Solution Chemistry, 23 (1994), pp. 105-120
DOI: 10.1007/bf00973540.

19. D.S. Abrams ,J.M. Prausnitz
Statistical thermodynamics of liquid mixtures: A new expression for the excess Gibbs energy of partly or completely miscible systems
AIChE Journal, 21 (1975), pp. 116-128
DOI: doi:10.1002/aic.690210115.

20. T.F. Anderson ,J.M. Prausnitz
Application of the UNIQUAC Equation to Calculation of Multicomponent Phase Equilibria. 1. Vapor-Liquid Equilibria
Industrial & Engineering Chemistry Process Design and Development, 17 (1978), pp. 552-561
DOI: 10.1021/i260068a028.

21. F. Dergal
Captage du CO_2 par les amines démixantes
University of Lyon 1, Lyon (2013)
Thesis

22. Y. Maham, A.E. Mather, L.G. Hepler
Excess Molar Enthalpies of (Water + Alkanolamine) Systems and Some Thermodynamic Calculations
Journal of Chemical & Engineering Data, 42 (1997), pp. 988-992
DOI: 10.1021/je960296h.

23. M. Mundhwa ,A. Henni
Molar excess enthalpy (HmE) for various {alkanolamine (1)+water (2)} systems at T=(298.15, 313.15, and 323.15)K
The Journal of Chemical Thermodynamics, 39 (2007), pp. 1439-1451
DOI: https://doi.org/10.1016/j.jct.2007.03.010.

24. H.A. Bruson ,C.W. MacMullen
Condensation of Phenols with Amines and Formaldehyde
Journal of the American Chemical Society, 63 (1941), pp. 270-272
DOI: 10.1021/ja01846a066.

25. A. Bondi ,H.L. Parry
Physical Properties of 2,4,6-Tri-(dimethylaminomethyl)-phenol Triacetate

The Journal of Physical Chemistry, 60 (1956), pp. 1406-1411
DOI: 10.1021/j150544a016.

List of Tables

Table 1. Suppliers and stated purities (mass fraction, *w*), of chemicals used in this study.

Pure component	Source	Mass fraction purity (certificate of analysis)	Purification method	Water Content (w_W %) (Karl Fisher)
DMP-30[a]	Sigma-Aldrich	0.972[b]	none	0.11
NaCl	Sigma-Aldrich	0.99	none	

[a] DMP-30 = 2,4,6-Tris(dimethylaminomethyl)phenol

[b] The major impurity in the studied compound is di(dimethylamino methyl) phenol . It was identified using liquid chromatography- mass spectroscopy.

Table 2.Comparison of experimental densities issued from the calibration and literature [8] densities (ρ^{exp} and ρ^{lit}) of aqueous solutions of sodium chloride (NaCl) as a function of temperature (T) at 0.1 MPa.

T	m_{NaCl}[a]	ρ_{NaCl}^{lit}	ρ_{NaCl}^{exp}
K	mol.kg^{-1}	g.cm^{-3}	
288.15	1.0147	1.0398	1.0398
	2.8577	1.1053	1.1053
298.15	1.0147	1.0368	1.0368
	2.8577	1.1011	1.1011
308.15	1.0147	1.0331	1.0331
	2.8577	1.0966	1.0964

[a] molality of sodium chloride solution in moles per kilogram of water

Standard uncertainty for experimental densities $u(\rho) = 1.10^{-5}$ g·cm^{-3}. Standard uncertainties are $u(p)$= 0.001 MPa, $u(T)$ = 0.03 K and $u(m_{NaCl})$ = 0.0001 mol.kg^{-1}

Table 3. Temperature (T) of liquid-liquid phase separation for {DMP-30 – water} system determined from the calorimetric and equillibrium cell techniques as a afunction of the molar fraction (x_a) at 0.1 MPa[a].

x_a	$u(x_a)$	T / K
microDSC		
0.0039	0.0004	332.55
0.0081	0.0008	322.95
0.015	0.002	318.25
0.024	0.003	317.25
0.033	0.004	317.35
0.0493	0.0002	318.35
0.0791	0.0003	319.45
0.1169	0.0004	322.45
0.1478	0.0005	325.75
0.195	0.0007	331.75
0.2923	0.0009	345.45
Equilibrium cell		
0.0283	0.0003	317.65
0.331	0.001	352.95

[a] $u(x_a)$ is the standard uncertainty for molar fraction.
Standard uncertainties are $u(p)$= 0.001 MPa and $u(T)$ = 2 K.

Table 4. Model parameters determined for the extended scaling law equation, the NRTL and UNIQUAC excess Gibbs energy models.

Model parameters							Temperature range (/K)
Extended scaling law equation[a]							
T_c	x_{ca}	B_1	B_2	B_3	A_1	A_2	317.5-353
317.5	0.0250	-0.027541	-1.91794	3.17011	3.66384	-5.99645	
NRTL[*,b]							
A_{12}^{NRTL}	A_{21}^{NRTL}	B_{12}^{NRTL}	B_{21}^{NRTL}	C_{12}^{NRTL}	C_{21}^{NRTL}	α	317.5-353
-45754.2	35505.8	253.842	-203.342	-0.358458	0.316699	0.2	
UNIQUAC[*,c]							
$A_{12}^{\mathrm{UNIQUAC}}$	$A_{21}^{\mathrm{UNIQUAC}}$	$B_{12}^{\mathrm{UNIQUAC}}$	$B_{21}^{\mathrm{UNIQUAC}}$	$C_{12}^{\mathrm{UNIQUAC}}$	$C_{21}^{\mathrm{UNIQUAC}}$		
-559.415	730.404	0.069182	0.232337	0.007075	-0.009806		295-313
r_1	r_2	q_1	q_2	q_1'	q_2'		
11.84	0.92	9.7	1.4	$q_1^{0.2}$	1.0		

[*] indices 1 and 2 used with NRTL and UNIQUAC model parameters, refer to amine and water, respectively.

[a] T_c = lower critical solution temperature; x_{ca} = molar fraction of the critical point; B_i and A_i are adjustable coefficients of the extended law equations 3a and 3b

[b] A_{ij}^{NRTL}, B_{ij}^{NRTL} and C_{ij}^{NRTL} are coefficients for NRTL model fit to equation 6

[c] A_{ij}^{NRTL}, B_{ij}^{NRTL} and C_{ij}^{NRTL} are coefficients for UNIQUAC model fit to equation 12;

r_i = volume parameter molecule i; q_i = surface parameter; q_i' = corrected surface parameter

Table 5. Densities (ρ_a) and specific heat capacities ($C_{p,a}$) for pure DMP-30 as a function of temperature at 0.1 MPa.

T / K	$c_{p,a}$ / J·g^{-1}·K^{-1}	ρ_a / g·cm^{-3}
288.15	_	0.986
298.15	1.93	0.978
308.15	1.96	0.973
318.15	2.01	0.962
328.15	2.06	0.955
338.15	2.09	0.946

[a] Standard relative uncertainties for specific heat capacity and density are $u_r(c_{p,a}) = 0.006$ and $u_r(\rho_a) = 0.005$. For heat capacity measurement, the standard uncertainties for temperature and pressure are $u(T) = 0.01$ K, $u(p) = 0.001$ MPa. For density, $u(T) = 0.03$ K and $u(p) = 0.001$ MPa.

Table 6. Molar heat capacities $C_{p,s}$ and excess molar heat capacities (C_p^E)for {DMP-30 – water} system and the standard uncertainties (u) as function of amine molar fraction x_a and temperature at 0.1 MPa[a].

x_a	$u(x_a)$	$C_{p,s}$	$u(C_{p,s})$	C_p^E	$u(C_p^E)$
		$J \cdot mol^{-1} \cdot K^{-1}$			
298.15 K					
0.0039	0.0004	79	1	2.2	1.0
0.0081	0.0008	83	1	4.5	1.1
0.015	0.002	90	1	7.8	1.2
0.024	0.003	99	1	11.9	1.5
0.033	0.004	106	1	14.9	1.9
0.0493	0.0002	117	1	19.8	1.0
0.0791	0.0003	134	2	25.9	2.0
0.1169	0.0004	156	2	30.6	2.0
0.1478	0.0005	173	2	32.9	2.0
0.1950	0.0007	200	2	34.9	2.0
0.2923	0.0009	253	3	35.8	3.0
308.15 K					
0.0039	0.0004	79	1	2.27	1.0
0.0081	0.0008	83	1	4.59	1.1
0.015	0.002	90	1	8.02	1.2
0.024	0.003	100	1	12.2	1.5
0.033	0.004	106	1	15.4	1.9
0.0493	0.0002	118	1	20.6	1.0
0.0791	0.0003	136	2	27.2	2.0
0.1169	0.0004	159	2	32.3	2.0
0.1478	0.0005	176	2	34.9	2.0
0.1950	0.0007	204	2	37.2	2.0
0.2923	0.0009	259	3	38.3	3.0

[a] $u(C_{p,s})$ is the standard uncertainty on isobaric heat capacity. $u(C_p^E)$ is the standard uncertainty on the excess capacities calculated using basic principles of error propagation. Standard uncertainties are on temperatire and pressure are $u(T)$ = 0.01 K, $u(p)$= 0.001 MPa.

Table 7. Densities ρ_s and excess molar volumes V^E for {DMP-30 – water} systems as function of amine molar fraction (x_a) and temperature at at 0.1 MPa[a].

x_a	$u(x_a)$	ρ_s	$u(\rho_s)$	V^E	$u(V^E)$
		g.cm^{-3}		cm^3.mol^{-1}	
288.15 K					
0.0031	0.0003	1.0013	0.0004	-0.05	0.01
0.0051	0.0003	1.0026	0.0004	-0.08	0.01
0.0131	0.0003	1.007	0.0004	-0.21	0.02
0.0226	0.0003	1.0109	0.0005	-0.35	0.03
0.0339	0.0003	1.0142	0.0005	-0.51	0.05
0.0464	0.0004	1.0166	0.0005	-0.67	0.06
0.0625	0.0003	1.0183	0.001	-0.85	0.09
0.091	0.001	1.0191	0.001	-1.11	0.13
0.0934	0.0004	1.0191	0.001	-1.13	0.13
0.1395	0.0005	1.0176	0.001	-1.44	0.19
0.1436	0.0005	1.0179	0.001	-1.49	0.20
0.1996	0.0008	1.0134	0.001	-1.64	0.28
0.247	0.001	1.0095	0.001	-1.67	0.35
0.2453	0.0007	1.0092	0.001	-1.63	0.34
0.298	0.002	1.0073	0.002	-1.78[b]	0.43
0.3382	0.0009	1.0039	0.002	-1.65	0.49
0.366	0.004	1.0022	0.002	-1.60	0.53
0.436	0.006	0.998	0.002	-1.36 [b]	0.65
0.4784	0.001	0.9968	0.002	-1.34	0.73
0.4836	0.001	0.9966	0.002	-1.32	0.73
0.498	0.009	0.9963	0.003	-1.32	0.76
0.57	0.01	0.9938	0.003	-1.12	0.90
0.62	0.01	0.9923	0.003	-0.96	1.00
0.74	0.02	0.9894	0.004	-0.58	1.25
0.8253	0.0006	0.9883	0.004	-0.42	1.46
298.15 K					
0.0031	0.0003	0.9988	0.0005	-0.05	0.01
0.0051	0.0003	0.9998	0.0005	-0.08	0.01
0.0131	0.0003	1.0033	0.0005	-0.20	0.02
0.0226	0.0003	1.0044	0.0005	-0.29	0.03
0.0339	0.0003	1.0063	0.0005	-0.42	0.05
0.0464	0.0004	1.0087	0.0005	-0.58	0.07
0.0625	0.0003	1.0104	0.0006	-0.76	0.09
0.091	0.001	1.0115	0.0007	-1.05	0.13
0.0934	0.0004	1.0116	0.0007	-1.07	0.13
0.1395	0.0005	1.0090	0.0008	-1.33	0.20
0.1436	0.0005	1.0095	0.0009	-1.39	0.20
0.1996	0.0008	1.005	0.001	-1.53	0.28

0.247	0.001	1.001	0.001	-1.60	0.35
0.2453	0.0007	1.001	0.001	-1.53	0.35
0.298	0.002	0.999	0.002	-1.68[b]	0.43
0.3382	0.0009	0.996	0.002	-1.58	0.50
0.366	0.004	0.994	0.002	-1.52	0.54
0.436	0.006	0.990	0.002	-1.31[b]	0.66
0.4784	0.001	0.989	0.002	-1.30	0.74
0.4836	0.001	0.989	0.002	-1.31	0.75
0.498	0.009	0.989	0.003	-1.31	0.77
0.57	0.01	0.986	0.003	-1.05	0.91
0.62	0.01	0.984	0.003	-0.92	1.01
0.74	0.02	0.981	0.004	-0.55	1.27
0.8253	0.0006	0.980	0.004	-0.42	1.48
308.15 K					
0.0031	0.0003	0.9955	0.0005	-0.05	0.01
0.0051	0.0003	0.9965	0.0005	-0.08	0.01
0.0131	0.0003	0.9995	0.0005	-0.19	0.02
0.0226	0.0003	1.002	0.0005	-0.32	0.03
0.0339	0.0003	1.0041	0.0005	-0.46	0.05
0.0464	0.0004	1.0055	0.0006	-0.60	0.07
0.0625	0.0003	1.0063	0.0006	-0.77	0.09
0.091	0.001	1.0061	0.0007	-1.01	0.13
0.0934	0.0004	1.006	0.0007	-1.02	0.13
0.1395	0.0005	1.004	0.0009	-1.32	0.20
0.1436	0.0005	1.0038	0.0009	-1.34	0.20
0.1996	0.0008	0.999	0.001	-1.47	0.29
0.247	0.001	0.996	0.001	-1.54	0.36
0.2453	0.0007	0.995	0.001	-1.48	0.35
0.298	0.002	0.993	0.002	-1.62[b]	0.44
0.3382	0.0009	0.990	0.002	-1.52	0.50
0.366	0.004	0.989	0.002	-1.47	0.55
0.436	0.006	0.985	0.002	-1.28 [b]	0.67
0.4784	0.001	0.984	0.002	-1.26	0.75
0.4836	0.001	0.984	0.002	-1.27	0.75
0.498	0.009	0.983	0.003	-1.25	0.78
0.57	0.01	0.981	0.003	-1.03	0.92
0.62	0.01	0.979	0.003	-0.89	1.02
0.74	0.02	0.976	0.004	-0.54	1.29
0.8253	0.0006	0.976	0.004	-0.43	1.50

[a] $u(x_a)$ ist he standard uncertainty on molar fraction, $u(\rho_s)$ is the standard uncertainty on density and $u(V^E)$ is the standard uncertainty on the excess molar volume. Standard uncertainties on temperature and pressure are $u(T)$ = 0.03 K, $u(p)$= 0.001 MPa.

[b] These values were omitted to determine Redlich-Kister equation parameters

Table 8. Redlich-Kister parameters a_i (Eq. 15) for {DMP-30 – water} system and standard error (σ) of the estimate at temperatures (T) range from 288.15 K to 308.15.

T / K	a_0	a_1	a_2	a_3	σ^a
288.15	-5.3417	-4.8826	-3.7095	-2.9257	0.04
298.15	-5.1325	-4.8394	-3.4536	-2.3634	0.05
308.15	-4.9463	-4.5915	-3.5095	-2.0641	0.04

[a] $\sigma = \sqrt{\sum_i^n \frac{\left(V_{i,exp}^E - V_{i,calc}^E\right)^2}{n-p}}$, with n and p the numbers of experimental and adjustable parameters, respectively.

List of Figures

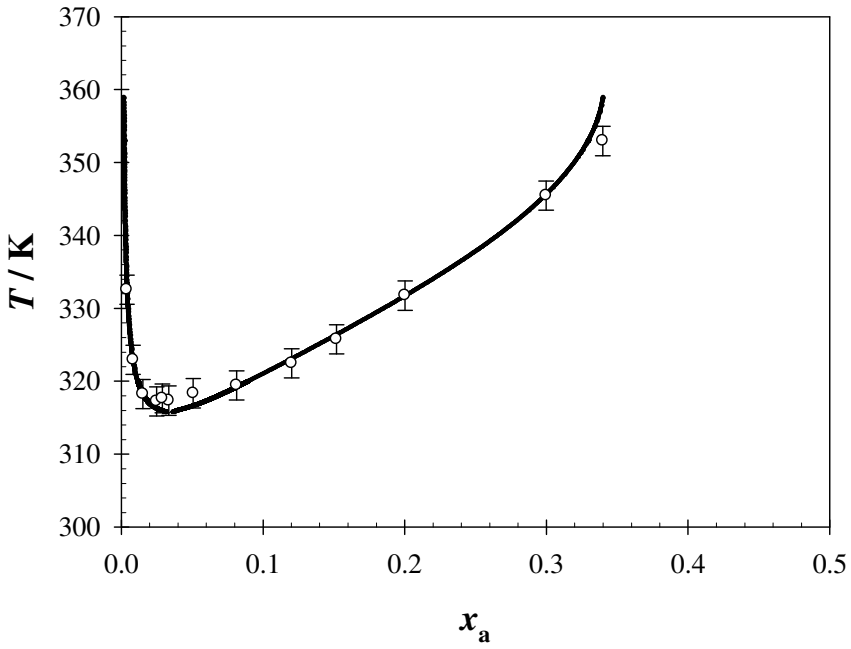

Figure 1. Liquid-liquid equilibrium diagram for {DMP-30 – water} system: ○, experimental data and full line, NRTL modeling.

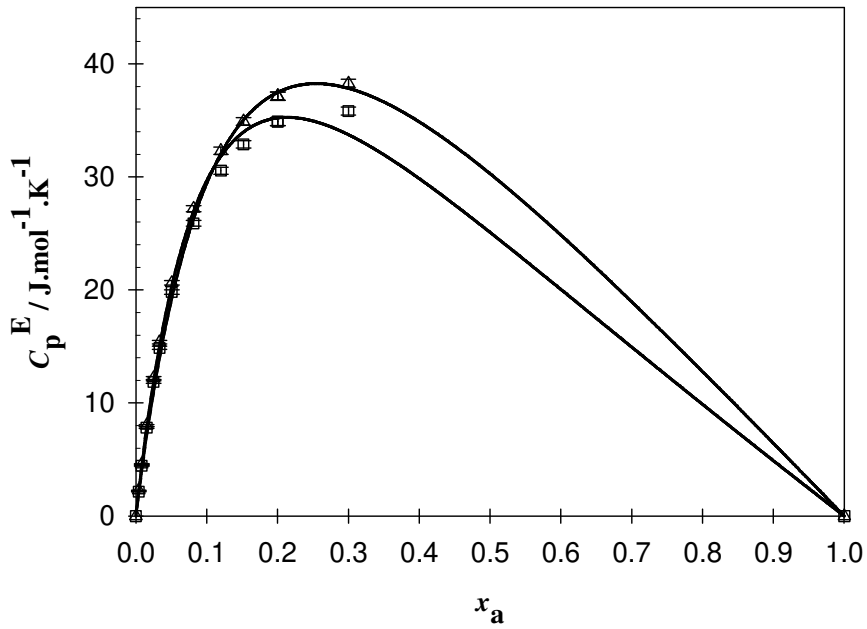

Figure 2. Excess molar heat capacities of {DMP30 – H_2O} system at 298.15 K (○) and 308.15 K (△).

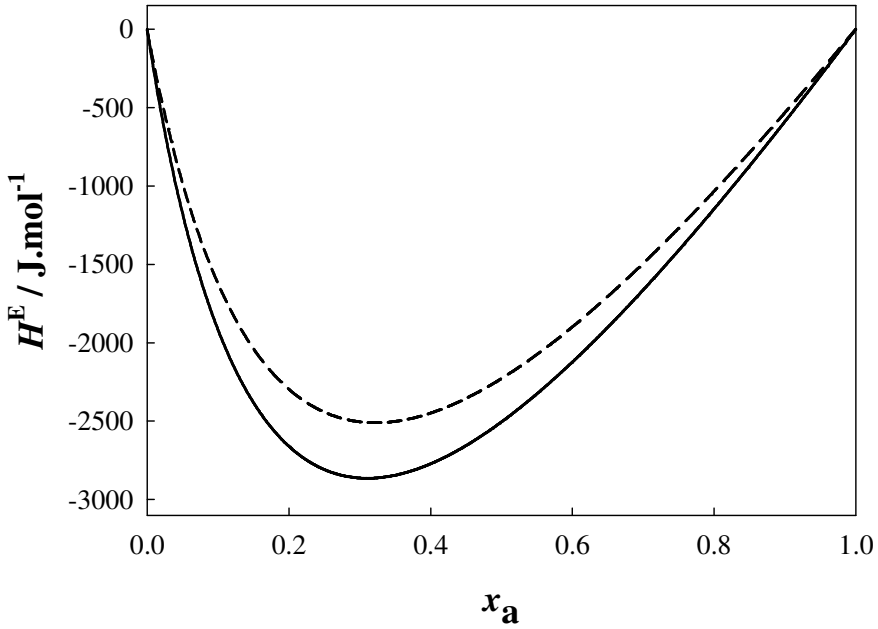

Figure 3. Predicted excess molar enthalpiess of {DMP30 – H_2O} system at 298.15 K (full line) and 308.15 K (dash line).

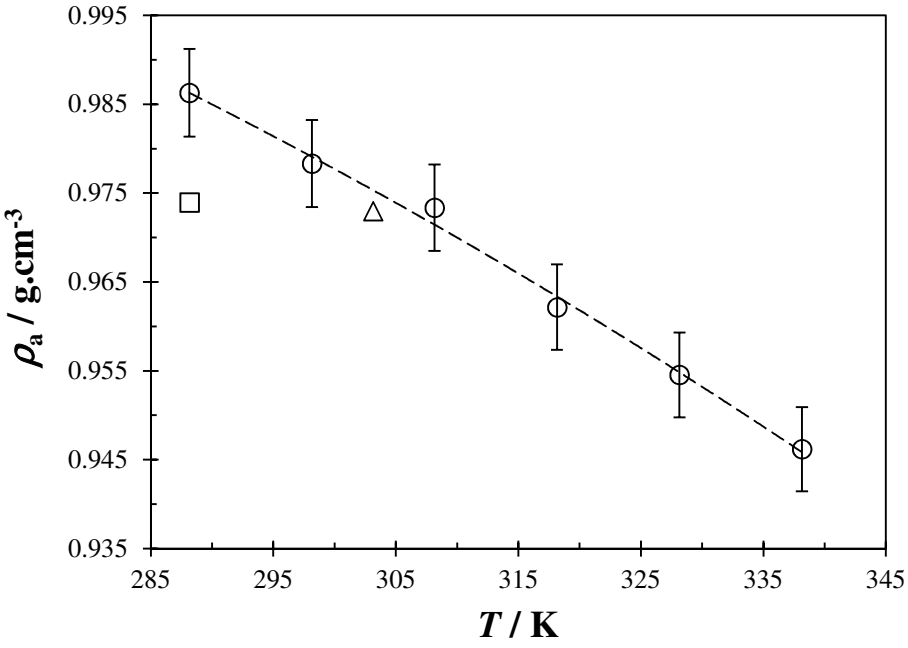

Figure 4. Comparison of densities of pure DMP-30 as function of temperature from this work with values available in the literarure: ○, this work; □, Bruson and MacMullen [24]; △, Bondi and Parry [25]. Dashed lines, connecting line.

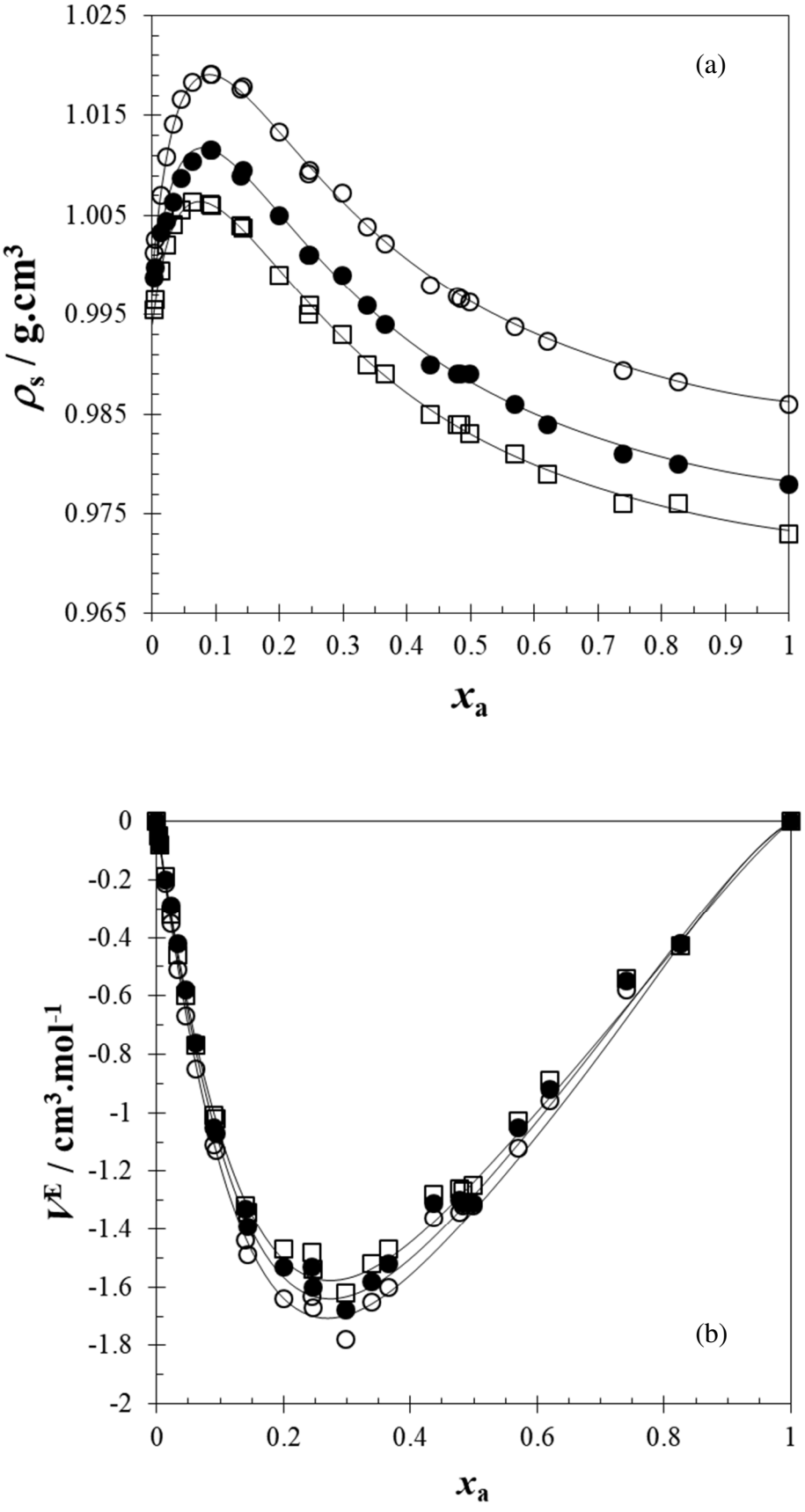

Figure 5. (a), densities ρ_s and (b), excess molar volumes V^E for {DMP-30 – water} system at 288.15 K (○), 298.15 K (●) and 308.15 K (□). Full line, Redlish-Kister equation.